Thermal Evolution of Chromium(III) Ions in Hydrotalcite-like Compounds

F. M. Labajos and V. Rives*

Departamento de Química Inorgánica, Universidad de Salamanca, 37008-Salamanca, Spain

Received December 28, 1995[⊗]

Hydrotalcite-like compounds containing Mg(II) and Cr(III) or Ni(II) and Cr(III) cations in the brucite-like layers have been synthesized by the coprecipitation method. The layered structure has been confirmed by Powder X-ray diffraction, and characterization has been completed by elemental chemical analysis, FT-IR and vis−UV/diffuse reflectance spectroscopies, and thermal analysis (differential thermal analysis and thermogravimetric analysis). The behavior shown during the thermal studies depends on the atmosphere used to carry out the study; a weak endothermic effect, at temperatures coinciding with a small weight loss, is recorded when the analysis is performed in air but not when performed in nitrogen, and so it is ascribed to oxidation processes. Formation of chromate-like species in the samples calcined at intermediate temperatures has been confirmed by powder X-ray diffraction for sample MgCr-HT and is suggested by FT-IR spectroscopy for sample NiCr-HT; the lack of success in identifying chromate-like species for sample NiCr-HT calcined at different temperatures by X-ray diffraction suggests that these species are very well dispersed. Their presence has been undoubtedly established by temperature-programmed reduction analysis of the samples, showing a maximum oxidation state of Cr ions (+6) when the sample is calcined at 623 K. Calcination at high temperatures leads to formation of MCr_2O_4 (M = Mg, Cr) spinel in addition to rock salt oxide of the divalent cation. Formation of amorphous materials at intermediate calcination temperature accounts for specific surface area development for these samples.

Introduction

Anionic clays with the hydrotalcite-like (HT) structure represent the counterpart of the well-known cationic clays. Their general formula can be written as $[M^{II}_{1-x}M^{III}_x(OH)_2]^{x+}[A^{n-}]_{x/n}\cdot mH_2O$—as water molecules also exists in the interlayers—where M = metal and A = anion. They consist of a brucite-like network where the divalent cations are partially subtituted by trivalent ones. In the brucite-like layers, each cation is octahedrally surrounded by hydroxides, the octahedra sharing edges to form two-dimensional sheets. These sheets carry an excess of positive charge due to the presence of M^{3+} and this is balanced by interlayer anions which bind the sheets together. The presence of different cations in the brucite-like layers, different anions in the interlayers, and different hydration degrees leads to isostructural solids with varying *a* and *c* crystallographic parameters and to polytopic crystals, depending on the packing sequence.[1,2] Thus, these compounds have received considerable attention, because of both industrial and academic interest, due to their potential applications as ion exchangers, adsorbents, and catalysts or catalyst supports.[3−6] Their thermal descomposition leads to mixtures of pure and mixed oxides that may recover the original layered structure upon rehydration in the presence of several anions and undergo transformation to highly reactive oxides (catalysts) upon calcination at high temperatures.[7] We here report on these materials, where Cr(III) has been introduced in the brucite-like layers of Mg(II) and Ni(II) hydroxides by isomorphic substitution. The study is extended to the nature of the products formed after thermal decomposition at high temperature, especially following the evolution of chromiun cations with the calcination temperature. Formation of Cr(VI)-containing compounds has been observed for materials calcined at intermediate temperatures.

Experimental Section

Synthesis. The hydrotalcite-like compounds were prepared by the coprecipitation method.[8] All chemicals used were from Fluka (p.a.). A 250 mL portion of a solution containing magnesium(II) or nickel(II) nitrate (0.5 M) and chromium(III) nitrate (0.25 M), i.e., with a molar M:Cr ratio = 2, was slowly added dropwise to 250 mL of a 1 M Na_2CO_3 solution in 3 M NaOH; this solution was magnetically stirred during addition of the former solution. During precipitation, CO_3^{2-} anions are incorporated into the hydrotalcite structure, as their affinity for the hydroxide ion is larger than that of other anions existing in the solution (nitrate and hydroxide).[9,10] The suspensions obtained were stirred at room temperature overnight and then further aged at 400 K for 11 days in a stainless steel digestion bomb lined with Teflon, in order to obtained better crystallized materials.[11] The powders were separated by centrifugation and washed repeatedly with deionized water until no indication of nitrate was observed by FT-IR spectroscopy and then filtered and dried in air at 350 K overnight. Calcined samples were prepared by heating these solids in air during 2 h at temperatures corresponding to formation of thermally stable phases (see below). Samples will be labeled as MgCr-HT or NiCr-HT, respectively, for parent solids containing Mg(II) and Cr(III) or Ni(II) and Cr(III). Calcined samples will be labeled as MCr-HT/X, where X stands for the calcination temperature, in kelvin.

Characterization. Chemical analysis for magnesium, nickel, and chromium was carried out by atomic absorption in a Mark-II ELL-240 instrument. Analysis for C and H was performed in a Perkin Elmer 2400 CHN apparatus.

* Author to whom all correspondence shoud be addressed. FAX: +34 23 29 45 15. E-mail: vrives@gugu.usal.es.

⊗ Abstract published in *Advance ACS Abstracts,* August 1, 1996.

(1) Booking, A. S.; Drits, V. A. *Clays Clay Miner.* **1993**, *41*, 551.
(2) Booking, A. S.; Cherkashim, V. I.; Drits, V. A. *Clays Clay Miner.* **1993**, *41*, 558.
(3) Reichle,W. T. *J. Catal.* **1985**, *94*, 547.
(4) Miyata, S. *Clay Clay Miner.* **1975**, *23*, 369.
(5) Drezdon, M. A. *Inorg. Chem.* **1988**, *27*, 4628.
(6) Occelli, M. L.; Landau, S. D.; Pinnavaia, T. J. *J. Catal.* **1984**, *90*, 256.
(7) Labajos, F. M.; Malet, P.; Rives, V.; Ulibarri, M. A. *3rd GIPS in Inorganic Chemistry*; Senigallia, Italy, 1995.
(8) Reichle, W. T. *Solid State Ionics* **1986**, *22*, 135.
(9) Miyata, S. *Clays Clay Miner.* **1983**, *31*, 305.
(10) Mendiboure, A.; Schöllhorn, R. *Rev. Chim. Miner.* **1986**, *43*, 819.
(11) Labajos, F. M.; Rives, V.; Ulibarri, M. A. *J. Mater. Sci.* **1992**, *27*, 1546.

S0020-1669(95)01648-X CCC: $12.00 © 1996 American Chemical Society

Table 1. Data from Chemical Analyses and Structural Formulas of the Compounds

	M[a]	Cr[a]	C[a]	H[a]	M:Cr[b]	formula
MgCr-HT	17.3	17.4	2.3	3.3	2.1	$[Mg_{0.68}Cr_{0.32}(OH)_2](CO_3)_{0.16}\cdot 0.86H_2O$
NiCr-HT	37.9	18.3	1.8	3.2	1.8	$[Ni_{0.65}Cr_{0.35}(OH)_2](CO_3)_{0.15}\cdot 0.99H_2O$

[a] Percent weight. [b] Atomic ratio.

Powder X-ray diffraction (PXRD) patterns were recorded on a Siemens D-500 diffractometer with a graphite-filtered Cu $K\alpha_1$ radiation (1.5405 Å) and interfaced to a DACO-MP data acquisition microprocessor provided with Diffract/AT software.

Differential thermal analysis (DTA) and thermogravimetric analysis (TG) of the samples were carried out in Perkin-Elmer DTA 1700 and TGS-2 apparatus, respectively, coupled to a Perkin-Elmer 3600 data station, at a heating rate of 10 K/min.

Specific surface areas were measured by the single-point method in a Micromeritics Flowsorb II-2300 apparatus by nitrogen adsorption after degassing the samples *in situ* at 400 K for 2 h.

The Fourier-transform infrared spectra (FT-IR) of the samples were recorded on a Perkin-Elmer FT-IR 1730 apparatus, having a nominal resolution of 2 cm^{-1} and averaging 100 scans; the sample was pressed in KBr pellets. The vis−UV spectra in the 1000−200 nm (10 000−50 000 cm^{-1}) range were recorded by the diffuse reflectance technique (vis−UV/DR), on a Shimadzu UV-240 instrument, using slits of 5 nm and MgO as reference.

Temperature-programed reduction (TPR) analysis was carried out in a Micromeritics TPR/TPD 2900 instrument, at a heating rate of 10 K/min and by using ca. 15 mg of sample and a H_2/Ar (5% by volume) mixture (from Sociedad Española del Oxígeno, Spain) as reducing agent (60 mL/min); experimental conditions for TPR runs were chosen according to data reported elsewhere[12] in order to achieve good resolution of the component peaks.

Results and Discussion

The M:Cr molar ratio in the starting solutions is maintained (±10%) in the solid obtained; see Table 1. However, the formulas of these samples cannot be determined solely from chemical analysis, due to the presence of interlayer water molecules. So, thermal analyses (see below) were performed. The solids synthesized show highly crystalline hydrotalcite-like structures. Figure 1 shows the PXRD patterns of the hydrotalcite-like samples. Sharp and narrow peaks are recorded, which can be ascribed to diffractions by (00l) planes, indicating that the material is formed by large, homogeneous particles. Indexing of the PXRD patterns indicates a hydrotalcite-like structure with polytypism 3R for both samples MgCr-HT and NiCr-HT. The good agreement between the values corresponding to successive diffractions by basal planes, i.e., $d(003) \approx 2d(006) \approx 3d(009)$, reveals highly packed stacks of brucite-like layers ordered along axis *c*. According to this polytypism, crystallographic dimensions of the crystals are $c = 22.92$ Å (i.e., $c = 3d(003)$) for sample MgCr-HT and $c = 22.50$ Å for sample NiCr-HT. The value of dimension *a* is calculated as twice the spacing corresponding to diffraction by planes (110),[13] i.e., a = 3.08 Å for sample MgCr-HT and a = 3.06 Å for sample NiCr-HT. The value of *d*(00l) depends solely of the thickness of the brucite-like layer and on the nature of the interlayer anion, carbonate in both samples here studied. However, dimension *a* depends on the ionic radii of the cations existing in the brucite-like layers and on the M(II)/M(III) substitution degree. The slightly lower value of dimension *a* for sample NiCr-HT than for sample MgCr-HT (3.06 vs 3.08 Å) can be due to the smaller ionic radius of Ni(II) ions (0.83 Å) than of Mg(II) ions (0.86 Å).[14]

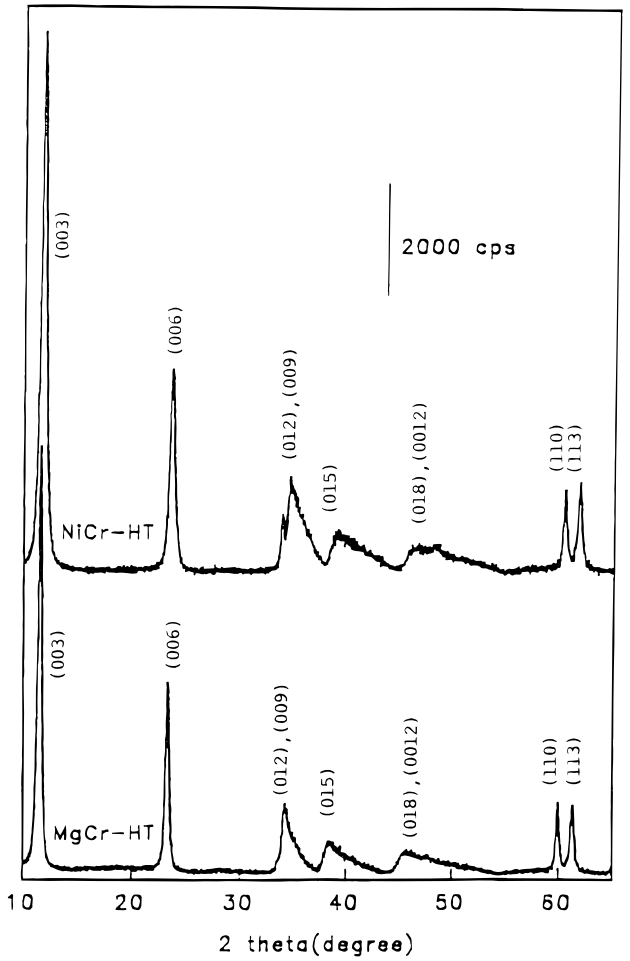

Figure 1. Powder X-ray diffraction patterns of MgCr-HT and NiCr-HT.

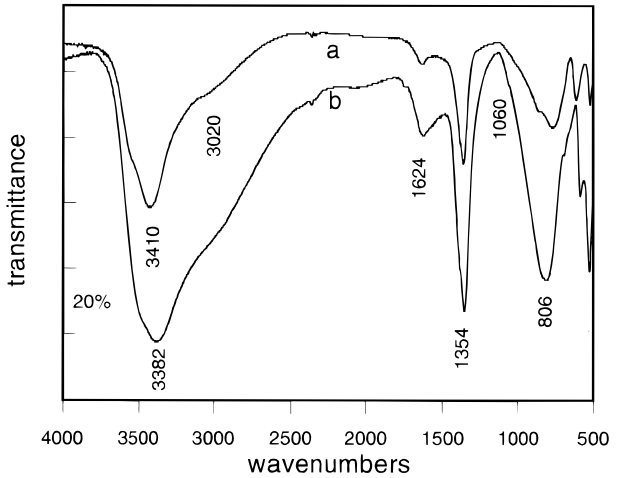

Figure 2. FT-IR spectra of (a) MgCr-HT and (b) NiCr-HT.

The FT-IR spectra are included in Figure 2. A strong, broad band centered at *ca.* 3400 cm^{-1}, is due to the stretching mode of hydrogen-bonded hydroxyl groups, both from the layers and from the interlayer water molecules. The bending mode of these water molecules, $\delta(H_2O)$, is responsible for the medium-intensity

(12) Malet, P.; Caballero, A. *J. Chem. Soc., Faraday Trans. I* **1988**, *84*, 2369.
(13) Cavani, F.; Trifiro, F.; Vaccari, A. *Catal. Today* **1991**, *11*, 171.
(14) Huheey, J. E.; Keiter, E. A.; Keiter, R. L. *Inorganic Chemistry: Principles of Structure and Reactivity*, 4th ed.; Harper Collins: New York, 1993.

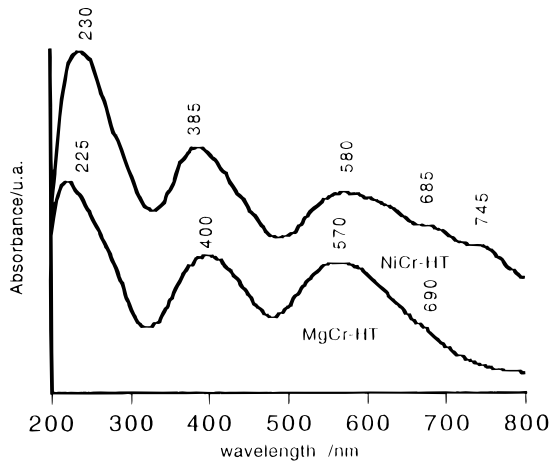

Figure 3. Vis−UV/DR spectra of MgCr-HT and NiCr-HT.

band recorded close to 1630 cm^{-1}. The easily detected shoulder close to 3020 cm^{-1} in both spectra is due to OH stretching of hydroxyl groups hydrogen-bonded to interlayer carbonate anions.[11] It should be noted that the main band at 3400 cm^{-1} and the shoulder at 3020 cm^{-1} are broader and stronger for sample NiCr-HT than for sample MgCr-HT. The sharp, intense band at 1360 ± 5 cm^{-1} is due to mode ν_3 of carbonate anions, shifted from its original value for free carbonate species because of the strong electrostatic interactions in the symmetry-restricted interlayer space. Such a lower symmetry gives rise also to activation of mode ν_1, originally forbidden in the IR, detected as weak shoulders at 1060 and 1077 cm^{-1} for samples NiCr-HT and MgCr-HT, respectively. Bands recorded below 800 cm^{-1} are due to M−O, M−O−M and O−M−O (M = Mg, Ni, Cr) modes.[15]

Vis−UV/DR spectra, Figure 3, show broad bands centered at the positions included in Table 1. The bands should originate from spin-allowed, Laporte-forbidden d−d transitions of Ni(II) and Cr(III) ions in an octahedral environment. The appreciable broadness of the bands can be, at least, partially due to the lower symmetry (D_{3d}) existing in the brucite-like layers, if compared to that of $M(H_2O)_6^{n+}$ species (O_h). According to ligand-field theory,[14] the ^4F ground state of Cr(III) ions (d^3) splits in an octahedral field into three states whose energies increase as $^4A_{2g}$ (ground state) < $^4T_{2g}$ < $^4T_{1g}$; in addition, state ^4P for the free ion remains unsplit as $^4T_{1g}$. So, three bands should be expected for Cr(III) ions in an octahedral environment. With regard to Ni(II), d^8, a similar situation should be expected, ground state ^3F for the free ion splitting into states $^3A_{2g}$ (ground state) < $^3T_{2g}$ < $^3T_{1g}$, and ^3P remains as $^3T_{1g}$. So, again, three spin-allowed, Laporte forbidden d−d transitions are expected, although the lowest energy band is usually split because of spin-orbit coupling. As a whole, up to six bands are expected for sample NiCr-HT but only three for sample MgCr-HT. As Cr(III) ions occupy octahedral sites in the brucite-like structure in both samples, the positions of the bands originating from d−d transitions in this ion should be rather close in both cases. Ascription of the bands to particular transitions has been made by starting from the spectrum for sample MgCr-HT (where only bands due to Cr(III) are expected) and then ascribing remaining bands in the spectrum of sample NiCr-HT to Ni(II) transitions. On the other hand, the environment of these cations in the brucite-like layers should be rather similar to that existing in the corresponding hexaaquo cations, for which bands are recorded at 17 400, 24 600, and 37 800 cm^{-1} for $[Cr(H_2O)_6]^{3+}$ and at 8500, 13 800, and 25 300 cm^{-1} for $[Ni(H_2O)_6]^{2+}$.[16]

Table 2. Vis−UV/DR-Recorded Absorption Bands for MgCr-HT and NiCr-HT and Their Ascription and Calculated Values for $10Dq_O$ and B (cm^{-1})

	MgCr-HT		NiCr-HT	
	Mg(II)	Cr(III)	Ni(II)	Cr(III)
charge transfer	44 400		43 500	
$^3A_{2g}(F) \rightarrow {}^3T_{1g}(P)$			26 000	
$^4A_{2g}(F) \rightarrow {}^4T_{1g}(F)$		25 000		24 100
$^4A_{2g}(F) \rightarrow {}^4T_{2g}(F)$		17 500		17 500
$^4A_{2g}(F) \rightarrow {}^2E_g$		14 500[a]		14 600[a]
$^3A_{2g}(F) \rightarrow {}^3T_{1g}(F)$			13 400	
$10Dq_O$		17 500	7 950	17 500
B		762	1 035	640

[a] "Ruby" line.

From comparison of the spectrum for sample MgCr-HT and that reported in the literature for $[Cr(H_2O)_6]^{3+}$, the absorptions at 17 500 and 25 000 cm^{-1} can be ascribed to the transitions $^4A_{2g}(F) \rightarrow {}^4T_{2g}(F)$ and $^4A_{2g}(F) \rightarrow {}^4T_{1g}(F)$, respectively. The position of the third band, corresponding to the transition $^4A_{2g}(F) \rightarrow {}^4T_{1g}(P)$, is not well defined because of the noticeable broadness of the band, probably overlapped with a charge transfer band, $OH^- \rightarrow M^{n+}$. From comparison of the spectra for samples MgCr-HT and NiCr-HT, the absorptions at 17 500 and 24 100 cm^{-1} in the latter sample should be due to the transitions $^4A_{2g}(F) \rightarrow {}^4T_{2g}(F)$ and $^4A_{2g}(F) \rightarrow {}^4T_{1g}(F)$, respectively.

The additional absorptions at 13 400 and 26 000 cm^{-1} in the spectrum of sample NiCr-HT should be then ascribed to the transitions $^3A_{2g}(F) \rightarrow {}^3T_{1g}(F)$ and $^3A_{2g}(F) \rightarrow {}^3T_{1g}(P)$, respectively, of Ni(II) ions. The first Ni(II) band is usually recorded below 10 000 cm^{-1}, and so it is outside the range of the spectrometer used in this work.

The positions of the third Cr(III) band (probably within the charge transfer absorption close to 200−240 nm) and of the first Ni(II) band can be calculated by using the equations of Dou[17] to determine the crystal field splitting energy (CSFE = Δ_O = 10 Dq_O) and the Racah parameter, B, for moieties $[Cr(OH)_6]$ and $[Ni(OH)_6]$.

The Dou equations for d^3 ions are

$$10Dq_O = \nu_1 \qquad \text{(Tsuchida's rule)} \tag{1}$$

$$B = (\nu_2 - 2\nu_1)(\nu_2 - \nu_1)/3(5\nu_2 - 9\nu_1) \tag{2}$$

$$\nu_3 = (15/2)B + 15Dq_O + (1/2)(225B^2 + 100(Dq_O)^2 - 180(Dq_O)B)^{1/2} \tag{3}$$

while for d^8 ions the formulas are

$$Dq_O = [9(\nu_2 + \nu_3) - (85(\nu_2 - \nu_3)^2 - 4(\nu_2 + \nu_3)^2)^{1/2}]/340 \tag{4}$$

$$B = (\nu_2 + \nu_3 - 30Dq_O)/15 \tag{5}$$

$$\nu_1 = 10Dq_O \tag{6}$$

The values calculated for $10Dq_O$ and B are also included in Table 2. From the calculated values for $10Dq_O$ and B, and from the positions of bands ν_1 and ν_2 (for Cr) and ν_2 and ν_3 (for Ni), the expected positions for bands ν_3 (for Cr) and ν_1 (for Ni) can

(15) Hernández-Moreno, M. J.; Ulibarri, M. A.; Rendón, J. L.; Serna, C. J. *Phys. Chem. Miner.* **1985**, *12*, 34.

(16) Sutton, D. *Espectros Electrónicos de los Complejos de los Metales de Transición*; Reverte: Barcelona, Spain, 1975.

(17) Dou, Y. *J. Chem. Educ.* **1990**, *67*, 134.

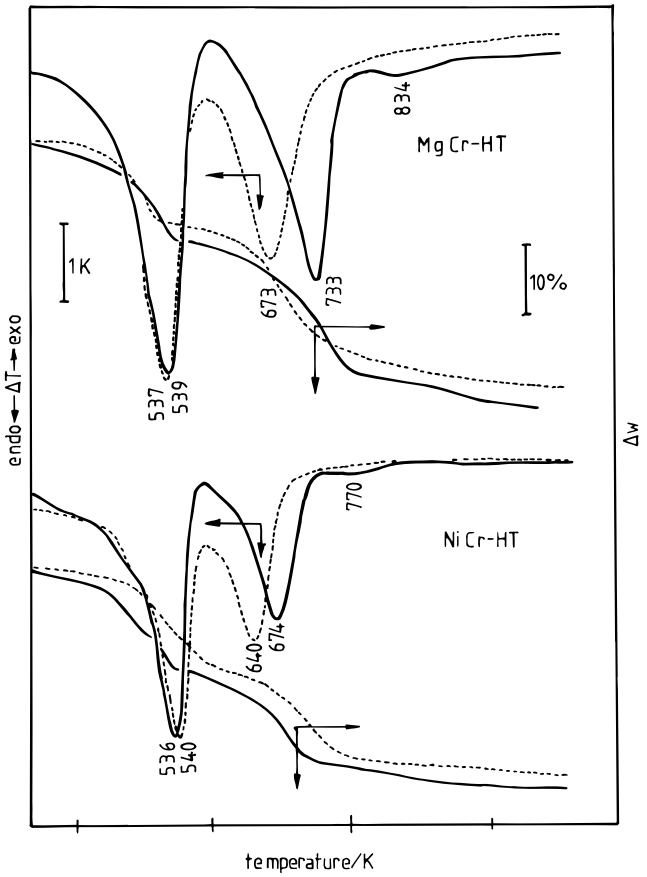

Figure 4. TG and DTA profiles of MgCr-HT and NiCr-HT recorded in air (solid lines) and in nitrogen (dotted lines).

be calculated using eqs 3 and 6, respectively. The values for ν_3 (Cr) were 39 100 and 38 200 cm^{-1}, respectively, for samples MgCr-HT and NiCr-HT, both values lying within the strong charge transfer absorption. For Ni, the value calculated for ν_1 was 7950 cm^{-1}, corresponding to 1258 nm, outside the wavelength range of the spectrometer used.

An additional, much weaker, band is recorded at 14 500−14 600 cm^{-1} in the spectra of samples MgCr-HT and NiCr-HT. This position is very close to that reported by Jørgensen for ruby, a solid solution of Cr(III) in α-Al_2O_3, where Cr(III) ions occupy octahedral holes.[18] This absorption arises from the spin-forbidden transition $^4A_{2g}(F) \rightarrow {}^2E_g$.

The TG and DTA profiles for these two samples are shown in Figure 4. Because of the presence of cations able to be oxidized during calcination, the analysis were performed both in air and in nitrogen, to distinguish the existence of oxidation processes. Broadly speaking, two strong endothermic effects are recorded in all cases. The pronounced asymmetry in the low-temperature side of the low-temperature DTA peak for sample NiCr-HT, together with the beginning of weight loss even from room temperature, is similar to that previously reported for hydrotalcite-like materials containing Ni(II) ions in the layers.[13] The DTA and TG profiles recorded in nitrogen are rather similar to those reported in the literature for hydrotalcite-like materials with nonoxidizable cations in the layers.[11,19−21] We previously showed[22] that the first endothermic peak, coinciding with the first weight loss, is due to removal of water molecules from the interlayer space, while the second weight loss, responsible as well for the second strong endothermic effect, is due to removal of water molecules (from condensation of hydroxyl groups from the brucite-like layers) and of carbon dioxide (from interlayer carbonate anions), thus leading to formation of mixed $M^{II}_xM^{III}_yO_z$ oxides. For sample MgCr-HT, the first peak is recorded at 539 K in air and at 537 K in nitrogen, while the second peak is recorded at 733 and 673 K, respectively, in air and nitrogen. Such a shift toward lower temperature when the analysis is performed in nitrogen is also observed for sample NiCr-HT, for which the first peak is recorded at 536 K (air) or 540 K (nitrogen) and the second peak shows its minimum at 674 K (air) or 640 K (nitrogen). Weight losses, recorded from the TG curves, were 16 and 19% in air and 14 and 23% in nitrogen for sample MgCr-HT and 15 and 14% in air and 15 and 16% in nitrogen for sample NiCr-HT, for the first and the second endothermic peaks, respectively. The amount of water molecules in the interlayer space can be calculated from the first weight loss recorded below *ca.* 600 K, and thus, the formulas shown in Table 1 for both samples can be concluded.

In addition to these two intense peaks, a weak, rather broad endothermic effect is recorded at 834 K (for sample MgCr-HT) and at 770 K (for sample NiCr-HT) when the analysis is performed in air, but these peaks are absolutely absent when the analysis is performed in nitrogen. A small weight loss is recorded in this same temperature range only when the analysis is performed in air, amounting *ca.* 4% for both samples. So, such an effect should be related to heat absorption during a chemical transformation involving oxidation/reduction processes.[13,23] It was previously claimed[13,24] that, during calcination in air of Cr(III)-containing hydrotalcites, oxidation occurs around 650−700 K, leading to collapsing of the layered structure at temperatures markedly below that required for hydrotalcites without oxidizable cations and forming chromates (or, at least, chromate-like compounds) which can be formulated as $MCrO_4$ (M = Mg, Ni). When the temperature is further increased, reduction to the tripositive state takes place, and the M−Cr spinel is formed. The Mg(II)−Cr(III) mixed oxide is more stable ($\Delta H° = -1783$ kJ mol^{-1}) than the Mg(II)−Cr(VI) mixed oxide ($\Delta H° = -1343$ kJ mol^{-1}), thus such a reduction accounting for the weak endothermic effect recorded in air, but not in nitrogen. Moreover, such a process takes place with O_2 removal, thus giving rise to a further weight loss. For our samples, the calculated weight loss (if all Cr has been assumed to be oxidized to the hexavalent state and then reduced again to Cr(III)) is *ca.* 3%, in agreement with the recorded value (4%).

To study in more detail the nature of the intermediate compounds formed during calcination of these samples, a portion of the solid was submitted to calcination in air for 2 h at temperatures corresponding to formation of thermally-stable phases, i.e., temperatures corresponding to a *plateau* in the DTA diagram, between two endo- or exothermic effects. Sample MgCr-HT was calcined at 573, 773, 1023, and 1273 K, and sample NiCr-HT was calcined at 513, 623, 723, and 973 K. Final calcination temperatures were selected sufficiently high to yield formation of well-crystallized phases, easily identified by PXRD.

(18) Jørgensen, C. K. *Adv. Chem. Phys.* **1963**, *5*, 33.
(19) Pesic, L.; Salipurovic, S.; Markovic, V.; Vucelic, D.; Kagunya, W.; Jones, W. *J. Mater. Chem.* **1992**, *2*, 1069.
(20) Labajos, F. M.; Rives, V.; Ulibarri, M. A. In *Multifuncional Mesoporous Inorganic Solids*; Sequeira, C. A. C., Hudson, M., Eds.; Kluwer Academic Publshers: Dordrecht, The Netherlanads, 1993.
(21) Yun, S. K.; Pinnavaia, T. J. *Chem. Mater.* **1995**, *7*, 348.
(22) Del Arco, M.; Martín, C.; Martín, I.; Rives, V.; Trujillano, R. *Spectrochim. Acta, Part A* **1993**, *49*, 1575.
(23) Clause, O.; Gazzano, M.; Trifiro, F.; Vaccari, A.; Zatorski, L. *Appl. Catal.* **1991**, *73*, 217.
(24) Cavani, F.; Clause, O.; Trifiro, F.; Vaccari, A. *Adv. Catal. Des.* **1991**, 186.

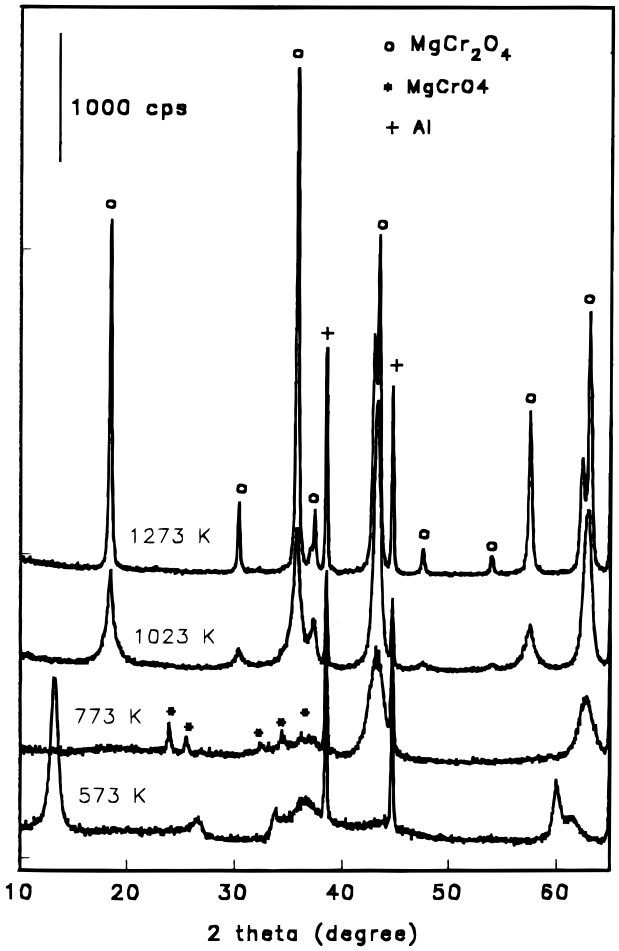

Figure 5. Powder X-ray diffraction patterns of MgCr-HT calcined in air at the temperatures given. Peaks noted "Al" arise from the sample holder.

The PXRD patterns of sample MgCr-HT calcined at the temperatures given are shown in Figure 5. The layered structure is still present after calcination at 573 K. Above this temperature (773 K), the characteristic peaks due to the layered material (specially peaks due to diffraction by planes (003) and (110)) are missing and, instead, in addition to two intense, broad peaks at 2.09 and 1.48 Å, due to poorly crystallized MgO, weak peaks are recorded in the 20−40° range (2θ), whose positions coincide with those of $MgCrO_4$ (file 21-1255).[25] Calcination at 1023 K cancels these peaks, and new ones develop, well resolved and sharper in the PXRD diagram of the sample calcined at 1273 K and corresponding to $MgCr_2O_4$ (file 10-351).[25]

It is highly surprising that these peaks due to formation of chromate-containing species are not recorded in the PXRD diagram of sample NiCr-HT calcined at the temperatures given above; probably the species are very well dispersed, thus making them undetectable by this technique. However, changes in the FT-IR spectra of these samples, Figure 6, should be related to formation of Cr(VI)-containing species. The band close to 1350 cm^{-1}, due to mode ν_3 of carbonate, is removed after calcination of the sample at 623 K, indicating collapsing of the layered structure at this temperature. At this same temperature, weak bands at 950 cm^{-1} (with a broad shoulder at lower wavenumbers) and 793 cm^{-1} develop and are recorded at 952, 906, 779, and 675 cm^{-1} for the sample calcined at 723 K. Free CrO_4^{2-} shows[26] an intense IR band at 865 cm^{-1} (ν_3, T_2), that shifts to 870 cm^{-1} for solid K_2CrO_4.[27] When the symmetry decreases, several bands are recorded for $K_2Cr_2O_7$ in the 970−850 cm^{-1} range. For $NiCrO_4$ these bands are recorded at 940, 782, and 690 cm^{-1}. Fuda et al.[28] report a broad, ill-structured absorption between 1000 and 800 cm^{-1}, characteristic of CrO_4^{2-} species. Although the positions of the bands reported in our work do not match exactly with the reported values, the shape of the spectrum and the number of bands resemble those reported for chromate species.

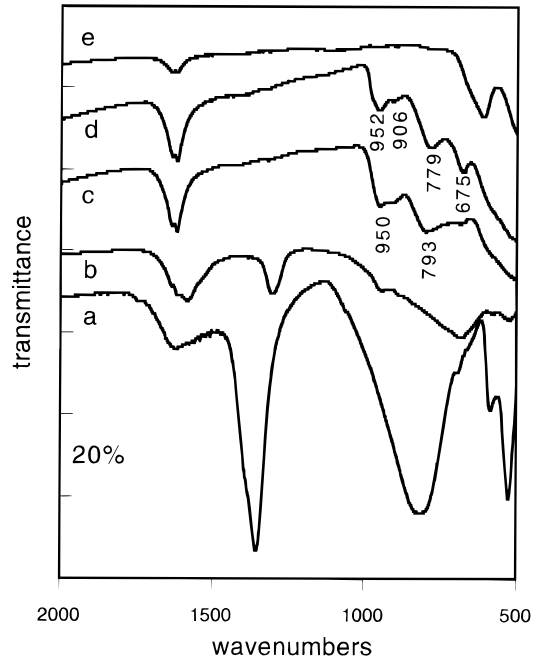

Figure 6. FT-IR spectra of (a) NiCr-HT subsequently calcined in air at (b) 513, (c) 623, (d) 723, and (e) 973 K.

Fuda et al.[28] suggest that the thermal activation process including the decomposition of carbonate may be related to oxidation of Cr(III) ions due to some potential ability of CO_3^{2-} for oxidation. When our sample is calcined at higher temperatures (973 K), the spectrum is rather similar to that previously reported for Cr_2O_3,[27] and the PXRD diagram shows[29] diffraction lines corresponding to formation of NiO and $NiCr_2O_4$, similarly that reported above for sample MgCr-HT calcined in this same temperature range.

In order to complete the study of the oxidation processes taking place during calcination of the samples, these have been submitted to TPR analysis. This technique has proved to be very valuable for the study of hydrotalcite-like materials containing oxidizable/reducible cations.[30] The TPR profiles of samples obtained upon calcination of sample NiCr-HT are shown in Figure 7; the profiles have been vertically displaced, for clarity. For sample NiCr-HT, a single reduction peak, with maximum at *ca.* 700 K, is recorded. This peak, slightly broader, but almost in the same temperature position, is recorded for all samples, although for sample NiCr-HT/973, this peak shifts toward higher temperatures and splits with two maxima at *ca.* 710 and 820 K. The shift and splitting are undoubtedly due to the fact that formation of well-crystallized phases after calcina-

(25) Joint Committe on Powder Diffraction Standards. *JCPDS File*; International Centre for Diffraction Data: Philadelphia, PA, 1977.
(26) Nakamoto, K. *Infrared and Raman Spectra of Inorganic and Coordination Compounds*, 4th ed.; J. Wiley & Sons: New York, 1986.
(27) Nyquist, R. A.; Kagel, R. O. *Infrared Spectra of Inorganic Compounds*; Acadmic Press: New York, 1971.
(28) Fuda, K.; Suda, K.; Matsunaga, T. *Chem. Lett.* **1993**, 1479.
(29) Labajos, F. M. Ph.D. Thesis. Universidad de Salamaca, Spain, 1993.
(30) Rives, V.; Ulibarri, M. A.; Montero, A. *Appl. Clay Sci.* **1995**, *10*, 83.

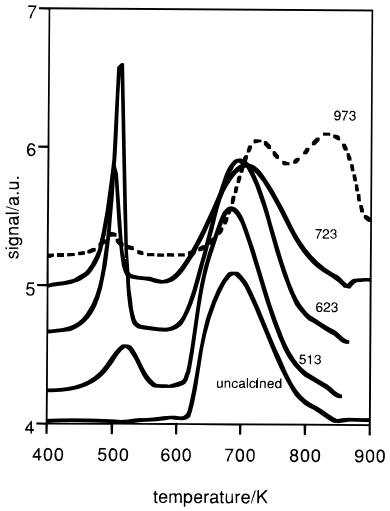

Figure 7. TPR profiles of NiCr-HT previously calcined at the temperatures given (in K).

tion at this temperature drastically changes the reduction patterns.[30] It has been previously shown[30] that Cr(III) is not reduced under the experimental conditions used in this work to carry out the TPR analysis. So, the peak at *ca.* 700 K in the reduction profile of sample NiCr-HT should be solely due to reduction of Ni(II) ions. Actually, taking into account the Ni content in this sample (6.44 mmol of Ni/g of sample; see Table 1) and the hydrogen consumption during its reduction (6.51 mmol of H_2/g of sample), it is concluded that hydrogen consumption corresponds to process

$$Ni^{2+} + H_2 \rightarrow Ni^0 + 2\,H^+$$

as the ratio between hydrogen consumption and nickel content equals 1.01. For samples obtained from NiCr-HT calcined at increasing temperatures, hydrogen consumption corresponding to the second reduction peak also coincides with the value expected for quantitative reduction of Ni(II) ions existing in these samples. However, the most striking feature of these profiles is the growth and then decrease of a rather sharp reduction peak slightly above 500 K. This peak is absent for the parent NiCr-HT sample and should then correspond to reduction of species different from Ni(II). Interlayer carbonate is not reduced under these experimental conditions,[30] and so this peak should correspond to processes that can be depicted as $Cr^{n+} \rightarrow Cr^{3+}$. Thus, taking into account the Cr content in these samples (as obtained from chemical analysis) and the hydrogen consumption corresponding to the reduction peak close to 500 K and assuming a final oxidation state for chromium after the TPR profiles of +3, the *average* oxidation state of chromium in the calcined samples can be obtained. Such average oxidation states were 3.55 (sample calcined at 513 K), 6.00 (623 K), 3.69 (723 K), and 3.14 (973 K); i.e., the chromium oxidation state passes through a maximum when the sample is calcined at 623 K and then decreases again. The temperature at which a maximum oxidation state is reached is not, as would be expected, below the temperature corresponding to the weak

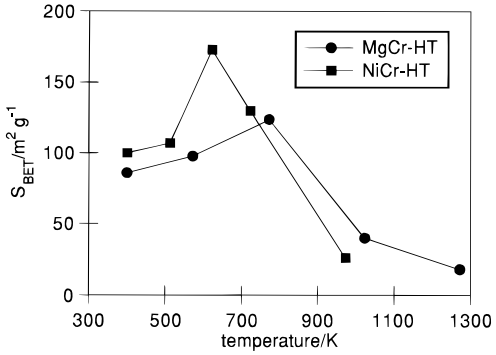

Figure 8. Change in the specific surface area values of MgCr-HT and NiCr-HT with the calcination temperature.

thermal effect (see DTA results above) ascribed to decomposition of the chromate-like species. However, it should be noted that the DTA is performed under continuous heating conditions, while to perform TPR experiments, samples were previously calcined for 2 h; therefore, kinetic effects (i.e., a lack of equilibrium during thermal analysis) cannot be discarded.

Figure 8 shows the evolution of the specific surface area of the sample, as determined by the BET method, with the calcination temperature. This evolution agrees with that observed for isostructural compounds.[20] Change in S_{BET} runs parallel to formation of amorphous solids, as concluded from PXRD analysis. The specific surface area increases for the calcined solids, reaching a maximum (124 and 173 $m^2\,g^{-1}$, respectively, for samples MgCr-HT and NiCr-HT) when the calcination is performed at 623−673 K, coinciding with formation of the most amorphous phases, as detected by PXRD; calcination at higher temperatures leads to a decrease in this value, as previously reported for hydrotalcites submitted to this same treatment.[11,20,31]

Conclusions

Thermal decomposition of Cr(III)-containing hydrotalcites at high temperature leads to formation of MO + MCr_2O_4 (M = Mg, Ni) mixtures, through intermediate formation of Cr(VI) species at relatively moderate temperatures, identified by powder X-ray diffraction, in the case of Mg,Cr-HT samples, although in Ni,Cr-HT samples these species should be very well dispersed, as they were not identified by PXRD. Temperature programmed reduction, however, confirms such an oxidation process, Cr ions reaching an average state of +6 when calcination is performed at 623 K.

Acknowledgment. Financial support from the CICYT (Grant MAT93-0787) and Consejería de Cultura y Turismo de la Junta de Castilla y León is gratefully acknowledged. We also thank Mr. A. Montero for his assistance in obtaining some of the experimental results.

IC951648T

(31) Del Arco, M.; Rives, V.; Trujillano, R. *Stud. Surf. Sci. Catal.* **1994**, *87*, 507.